

Imitation Learning for Robust and Safe Online Motion Planning: A Contraction Theory Approach

Hiroyasu Tsukamoto and Soon-Jo Chung

Abstract—This paper presents Learning-based Autonomous Guidance with Robustness, Optimality, and Safety guarantees (LAG-ROS), a real-time robust motion planning algorithm for safety-critical nonlinear systems perturbed by bounded disturbances. The LAG-ROS method consists of three phases: 1) Control Lyapunov Function (CLF) construction via contraction theory; 2) imitation learning of the CLF-based robust feedback motion planner; and 3) its real-time and decentralized implementation with a learning-based model predictive safety filter. For the CLF, we exploit a neural-network-based method of Neural Contraction Metrics (NCMs), which provides a differential Lyapunov function to minimize an upper bound of the steady-state Euclidean distance between perturbed and unperturbed system trajectories. The NCM ensures the perturbed state to stay in bounded error tubes around given desired trajectories, where we sample training data for imitation learning of the NCM-CLF-based robust centralized motion planner. Using local observations in training also enables its decentralized implementation. Simulation results for perturbed nonlinear systems show that the LAG-ROS achieves higher control performance and task success rate with faster execution speed for real-time computation, when compared with the existing real-time robust MPC and learning-based feedforward motion planners.

Index Terms—Machine Learning for Robot Control, Robust/Adaptive Control, Optimization and Optimal Control.

I. INTRODUCTION

In the near future of aerospace and robotic exploration on land, in water, and in deep space, teams of robots are expected to perform complex decision-making tasks autonomously in extreme environments, where their motions are governed by nonlinear dynamical systems with unknown external disturbances. In order for such operations to be successful, the agents are required to compute 1) an optimal target trajectory for the given nonlinear system, and 2) a feedback control input which *robustly* guarantees (exponential) convergence to the trajectory, both in real-time with their limited on-board computational resources. The objective of this work is to propose a learning-based autonomous guidance and control algorithm that meets these challenging requirements.

Related Work: Learning-based guidance and control designs of nonlinear systems have been an emerging area of research with the rise of neural networks and reinforcement learning [1], [2]. These techniques can be categorized into model-free and model-based methods, where each of them has pros and cons. The former approach is supposed to

learn desired optimal policies which work robustly as it uses training data obtained in real-world environments. This in turn implies that these techniques are not suitable for situations where sampling large training datasets is difficult as in aerospace and robotics systems. Also, proving stability and robustness properties of such model-free systems is challenging in general, although some techniques do exist [3], [4]. In contrast, the latter approach allows us to sample as much data as we want using a given dynamical system model, thereby constructing optimal policies using reinforcement learning [5], [6], imitation learning [7], [8], or both [9]–[11]. However, the learnt controller could yield cascading errors in the real-world environment if the nominal model poorly represents the true underlying dynamics [12].

Control theoretical approaches to circumvent such difficulties include robust Model Predictive Control (MPC) [13] equipped with a feedback control law for stability certificates, i.e., $u = k(x, x_d, u_d, t)$, where (x_d, u_d) is a target trajectory given by the tube-based MPC and $k(\cdot)$ is a feedback control policy that guarantees $x \rightarrow x_d$ for perturbed systems [14]. In [15], a differential feedback control law is proposed to guarantee tracking to any feasible nominal target trajectory given by existing motion planners for nonlinear systems including [16]–[19]. Since these frameworks explicitly use the knowledge of the desired states x_d for robustness properties to keep the system trajectories in a safe invariant tube around x_d even under external disturbances, they can provide provably stable and optimal control inputs at each time instant unlike most of learning-based control frameworks. One drawback is that they assume the existence of either a real-time implementable motion planning algorithm or a stabilizing tracking controller (e.g. Control Lyapunov Function (CLF) [20]–[22]) of given nonlinear systems, which is not always the case for practical applications.

Contributions: Therefore, in this study, we present Learning-based Autonomous Guidance with Robustness, Optimality, and Safety guarantees (LAG-ROS) as a novel way to bridge the gap between the learning-based and robust MPC-based motion planning techniques. In particular, the LAG-ROS requires only one neural network evaluation to get an optimal control input, which imitates the CLF-based robust feedback control policy. Since it explicitly models the robust policy $x \mapsto u$ implicitly accounting for target trajectories (x_d, u_d) , instead of a feedforward control policy $x_d \mapsto u_d$ given by existing motion planners [16]–[18], the LAG-ROS attains high control performance even under unknown external disturbances. Although we consider bounded disturbances in this paper, stochastic disturbances and parameter

The authors are with the Graduate Aerospace Laboratories, California Institute of Technology, Pasadena, CA, {htsukamoto, sjchung}@caltech.edu.

Code: <https://github.com/astrohiro>.

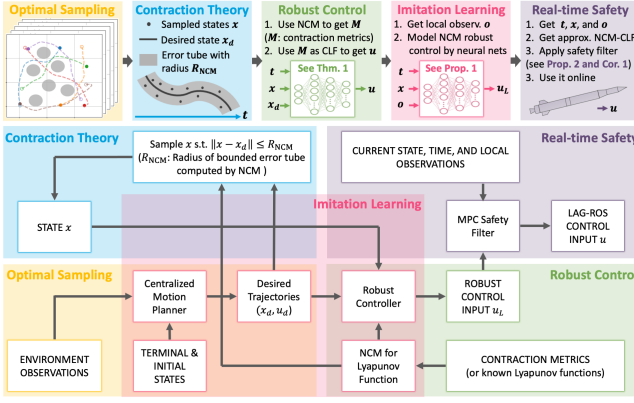


Fig. 1. Illustration of LAG-ROS.

uncertainty could be handled similarly using [23], [24]. Further, we propose one explicit way to construct a CLF for any general nonlinear systems in the LAG-ROS framework using a Neural Contraction Metric (NCM) [25], which is a learning-based optimal contraction metric designed to minimize an upper bound of the steady-state Euclidean distance between perturbed and unperturbed system trajectories [26]. We also delineate how to implement it in a distributed way and guarantee safety even for perturbed nonlinear systems, using the global-to-local autonomy synthesis [27] and MPC-based safety filter [8], respectively. Note that existing system identification and adaptive control techniques including [24], [28] could be used to obtain a more accurate description of the underlying dynamical system, for the sake of less-conservative application of the LAG-ROS. The architecture of the proposed framework depicted in Fig. 1 is summarized as follows.

In the offline phase, we first construct an NCM as described in [23]–[25], and utilize it as a CLF to design a robust optimal feedback control law. Since the NCM-CLF control ensures the system state to stay in bounded error tubes around x_d sampled by existing motion planners including the one used in this work [17], [18], we then sample state x and the NCM-CLF robust control u in these tubes for imitation learning of $x \mapsto u$. We also show that a known Lyapunov function based on a special structure of underlying dynamical systems can be used in the LAG-ROS framework, taking Lagrangian systems [29] as an example. In the online phase, we implement it by evaluating one neural network at each time instant, using the decentralization technique [8], [30] and the safety filter [27] on top the learnt robust control. It is demonstrated that the LAG-ROS outperforms existing real-time motion planning frameworks [8], [16]–[18] in cartpole balancing [31], motion planning and collision avoidance of multiple spacecraft simulators [32] in a cluttered environment, and autonomous reconfiguration of multiple spacecraft in Low Earth Orbit (LEO) [17]. In particular, the LAG-ROS requires less than 0.1s for real-time computation in all of these tasks, and achieves higher control performance and task success rate when compared with the existing real-time robust MPC and learning-based feedforward motion

planners.

Notation: For a vector $x \in \mathbb{R}^n$ and a matrix $A \in \mathbb{R}^{n \times m}$, we let $\|x\|$, δx , and $\|A\|$, denote the Euclidean norm, infinitesimal variation of x , and induced 2-norm, respectively. For a square matrix A , we use the notation $A \succ 0$, $A \succeq 0$, $A \prec 0$, and $A \preceq 0$ for the positive definite, positive semi-definite, negative definite, negative semi-definite matrices, respectively, and $\text{sym}(A) = (A + A^T)/2$. Also, $I \in \mathbb{R}^{n \times n}$ denotes the identity matrix.

II. ROBUST AND OPTIMAL TRACKING CONTROL USING NEURAL CONTRACTION METRICS

We first propose a novel feedback control framework for general nonlinear systems, which guarantees robustness, optimality, and stability when a target trajectory (x_d, u_d) is given. In particular, we use the Neural Contraction Metric (NCM) [25] when the Lyapunov function of a given nonlinear system is unknown. We also investigate the case where we know a Lyapunov function candidate, taking Lagrangian systems as an example.

A. Neural Contraction Metrics as Lyapunov Functions

The NCM is a recently developed deep learning-based design framework for constructing an optimal Lyapunov function for provably stable feedback control and estimation of nonlinear systems given as $\dot{x}(t) = f(x(t), t) + d(x, t)$, where $\bar{d} = \sup_{x,t} \|d(x, t)\| < +\infty$ [25]. This section presents the NCM Control Lyapunov Function (NCM-CLF) for designing an optimal robust control law, which guarantees exponential stability with respect to a given target trajectory (x_d, u_d) . We consider the following nonlinear dynamical system with a controller $u \in \mathbb{R}^m$:

$$\dot{x} = f(x, t) + B(x, t)u + d(x, t), \quad \dot{x}_d = f(x_d, t) + B(x_d, t)u_d \quad (1)$$

where $t \in \mathbb{R}_{\geq 0}$, $x, x_d: \mathbb{R}_{\geq 0} \mapsto \mathbb{R}^n$, $u_d: \mathbb{R}^n \times \mathbb{R}_{\geq 0} \mapsto \mathbb{R}^m$, $f: \mathbb{R}^n \times \mathbb{R}_{\geq 0} \mapsto \mathbb{R}^n$, and $B: \mathbb{R}^n \times \mathbb{R}_{\geq 0} \mapsto \mathbb{R}^{n \times m}$. The objective of this section is to find a robust optimal feedback control law $u = k(x, x_d, t)$ given x_d and $u_d(x_d, t)$ for the system (1). The following lemma is useful for this purpose.

Lemma 1: Consider a general feedback controller u defined as $u = k(x, x_d, t)$ with $k(x_d, x_d, t) = u_d(x_d, t)$, where $k: \mathbb{R}^n \times \mathbb{R}^n \times \mathbb{R}_{\geq 0} \mapsto \mathbb{R}^m$. If k is piecewise continuously differentiable, then $\exists K: \mathbb{R}^n \times \mathbb{R}^n \times \mathbb{R}_{\geq 0} \mapsto \mathbb{R}^{m \times n}$ s.t. $u = k(x_d, x_d, t) + K(x, x_d, t)(x - x_d)$.

Proof: We have $u = u_d + (k(x, x_d, t) - k(x_d, x_d, t))$ due to $k(x_d, x_d, t) = u_d(x_d, t)$. Since $k(x, x_d, t) - k(x_d, x_d, t) = \int_0^1 (dk(cx + (1-c)x_d, x_d, t)/dc)dc$, choosing K as $\int_0^1 (\partial k(cx + (1-c)x_d, x_d, t)/\partial x)dc$ gives the desired relation. ■

Lemma 1 implies that designing optimal k of $u = k(x, x_d, t)$ reduces to designing optimal $K(x, x_d, t)$ of $u = u_d(x_d, t) - K(x, x_d, t)(x - x_d)$. For such u , the virtual system of (1), which has $y = x, x_d$ as its particular solutions, is given as follows:

$$\dot{y} = \dot{x}_d + (A(x, x_d, t) + B(x, t)K(x, x_d, t))(y - x_d) + d_e(y, t) \quad (2)$$

where A is the State-Dependent Coefficient (SDC) form of the dynamical system (1) given by Lemma 2 of [23], i.e., $A(x, x_d, t)(x - x_d) = f(x, t) + B(x, t)u_d - f(x_d, t) - B(x_d, t)u_d$, and d_e satisfies $d_e(x, t) = d(y, t)$ and $d(x_d, t) = 0$.

Theorem 1: Suppose that f and B are piecewise continuously differentiable, and let $B = B(x, t)$ and $A = A(x, x_d, t)$ in (2) for notational simplicity. Consider a neural network trained to perfectly model the optimal contraction metric $M(x, x_d, t) = W(x, x_d, t)^{-1} \succ 0$ (Neural Contraction Metric (NCM)), given by the following convex optimization problem [24], [25]:

$$J_{CV}^* = \min_{\chi \in \mathbb{R}, \bar{W} > 0} \frac{\bar{d}\chi}{\alpha} \quad \text{s.t. (4) and (5).} \quad (3)$$

with the convex constraints (4) and (5) given as

$$\begin{aligned} -\dot{\bar{W}} + 2\text{sym}(A\bar{W}) - 2\nu BR^{-1}B^\top &\preceq -2\alpha\bar{W}, \quad \forall x, x_d, t \quad (4) \\ I &\preceq \bar{W}(x, x_d, t) \preceq \chi I, \quad \forall x, x_d, t \quad (5) \end{aligned}$$

where $\alpha, \underline{\omega}, \bar{\omega} > 0$, $\chi = \bar{\omega}/\underline{\omega}$, $\bar{W} = \nu W$, $\nu = 1/\underline{\omega}$, and $R = R(x, x_d, t) \succ 0$ is a given weight matrix on the control input u . Suppose also that the dynamics (1) is controlled by $u = u_d + K^*(x, x_d, t)e$, where $e = x - x_d$ and K^* is given by the following convex optimization-based controller for (x, x_d, t) :

$$\begin{aligned} K^* &= \arg \min_{K \in \mathbb{R}^{m \times n}} \|u - u_d\|^2 = \arg \min_{K \in \mathbb{R}^{m \times n}} \|K(x, x_d, t)e\|^2 \quad (6) \\ \text{s.t. } \dot{M} + 2\text{sym}(MA + MK(x, x_d, t)) &\leq -2\alpha M. \quad (7) \end{aligned}$$

Then (6) is always feasible, i.e., $V = \delta y^\top M \delta y$ is a CLF for y in (2), and minimizes the deviation of u from u_d under the stability constraint (7). Furthermore, we have that

$$\|x(t) - x_d(t)\| \leq \mathcal{R}(0)\sqrt{\bar{\omega}}e^{-\alpha t} + \frac{\bar{d}}{\alpha}\sqrt{\frac{\bar{\omega}}{\underline{\omega}}} = R_{\text{NCM}}(t) \quad (8)$$

where $\mathcal{R}(t) = \int_{x_d}^x \|\Theta(x(t), x_d(t), t)\delta y(t)\|$ for $M = \Theta^\top \Theta$. The metric M minimizes the steady-state upper bound of (8), and we call (6) the NCM-CLF control.

Proof: Let us first show that (6) is always feasible. Since the virtual dynamics is given as $\delta \dot{y} = (A - BK)\delta y$ for $d_e = 0$ in (2), we have for $K = -R^{-1}B^\top M$ that $\dot{V} = \delta y^\top (\dot{M} + 2\text{sym}(MA) - MBR^{-1}B^\top M)\delta y = \nu^{-1}\delta y^\top M(-\dot{\bar{W}} + 2\text{sym}(A\bar{W}) - 2\nu BR^{-1}B^\top)M\delta y$. Thus, the condition (4) ensures that (7) is feasible for $K = -R^{-1}B^\top M$. Also, for systems perturbed by d_e as in (2), the controller (6) gives $\dot{V} \leq -2\alpha V + 2\delta y^\top M \delta d_e$, resulting in $\dot{\mathcal{R}} \leq -\alpha \mathcal{R} + \bar{d}/\sqrt{\bar{\omega}}$ due to (5). The comparison lemma [22] with (5) yields (8). Further, Lemma 1 indicates that (6) minimizes the deviation of u from u_d under the stability constraint (7) without loss of generality. The optimality of M follows from Corollary 1 of [25]. ■

Remark 1: Although a neural network is used to model M in Theorem 1, we could directly solve the convex optimization at the expense of computational efficiency [33]. Also, one can select other performance-based objective functions in (3) and (6) depending on their application of interest, as described in [23], [33].

B. Dynamical Systems with Known Lyapunov Functions

There are several science and engineering applications where we know a Lyapunov function candidate of a given nonlinear system, one of which is a feedback linearizable system [22], [29], [34]. In this section, we illustrate how to construct robust tracking control for such systems, taking Lagrangian systems as an example.

Consider the following system with a bounded disturbance $d(x, t)$:

$$H(q)\dot{q} + C(q, \dot{q})\dot{q} + G(q) = u + d(x, t) \quad (9)$$

where $q: \mathbb{R}_{\geq 0} \rightarrow \mathbb{R}^n$, $u: \mathbb{R}_{\geq 0} \rightarrow \mathbb{R}^n$, $H: \mathbb{R}^n \rightarrow \mathbb{R}^{n \times n}$, $C: \mathbb{R}^n \times \mathbb{R}^n \rightarrow \mathbb{R}^{n \times n}$, $G: \mathbb{R}^n \rightarrow \mathbb{R}^n$, and $d: \mathbb{R}^n \times \mathbb{R}_{\geq 0} \rightarrow \mathbb{R}^n$ with $\bar{d} = \sup_{x, t} \|d(x, t)\| < +\infty$ and $x = [q^\top, \dot{q}^\top]^\top$. We note that the matrix $C(q, \dot{q})$ is selected to make $\dot{H} - 2C$ skew-symmetric, so we have a useful property s.t. $z^\top (\dot{H} - 2C)z = 0$, $\forall z \in \mathbb{R}^n$.

Theorem 2: Suppose that (9) is controlled by

$$u = u_n = H(q)\ddot{q}_r + C(q, \dot{q})\dot{q}_r + G(q) - K_\ell(t)s \quad (10)$$

where $\dot{q}_r = \dot{q}_d - \Lambda(q - q_d)$, $s = \dot{q} - \dot{q}_r$, $K_\ell \succ 0$, and $\Lambda \succ 0$. If K_ℓ , Λ , $\varepsilon > 0$ are selected so that $\exists \alpha > 0$ s.t. $\begin{bmatrix} 2K_\ell & -\varepsilon I \\ -\varepsilon I & 2\Lambda \end{bmatrix} \preceq -2\alpha M$, where $M = \Theta^\top \Theta = \text{diag}(H, \varepsilon I)$, then we have that

$$\|x - x_d\| \leq \frac{1}{\sqrt{P}} \left(\mathcal{R}(0)e^{-\alpha t} + \frac{\bar{d}}{\alpha} \frac{1}{\sqrt{m}} \right) = R_{\text{NCM}}(t) \quad (11)$$

where $x_d = [q_d^\top, \dot{q}_d^\top]^\top$, $\mathcal{R}(t) = \int_0^t \|\Theta(q(t))\delta y(t)\|$, $\xi = [s^\top, e^\top]^\top$, $e = x - x_d$, $mI \preceq M$, $P = \begin{bmatrix} \Lambda H \Lambda + \varepsilon I & \Lambda H \\ H \Lambda & H \end{bmatrix} \succ 0$, $\underline{P}I \preceq P$, and y is the state of the virtual system of (9), which has $[s^\top, e^\top]^\top$ and $[0^\top, 0^\top]^\top$ as its particular solutions.

Proof: For the virtual system defined as $H\dot{y}_1 + Cy_1 + K_\ell y_1 = d_s(y, t)$ and $\dot{y}_2 = y_1 - \Lambda y_2$, we have $y = [y_1^\top, y_2^\top]^\top = \xi = [s^\top, e^\top]^\top$ and $y = 0$ as its particular solutions when $d_s(\xi, t) = d(x, t)$ and $d_s(0, t) = 0$. Thus using a differential Lyapunov function $V = \delta y^\top M \delta y$, we can show that $\dot{\mathcal{R}} \leq -\alpha \mathcal{R} + \bar{d}/\sqrt{m}$ under the condition of this theorem [29], [35]. Since we have $\xi^\top M \xi = x^\top P x$ by definition, applying the comparison lemma [22] yields the desired relation. ■

Remark 2: The control parameters K_ℓ and Λ in Theorem 2 could also be optimized using the same technique in Theorem 1 or the one in Remark 1 [33].

III. IMITATION LEARNING OF ROBUST OPTIMAL MOTION PLANNERS

Although the NCM-CLF control of Theorem 1 guarantees exponential stability and is robust against external disturbances, it requires online computation of an optimal target trajectory (x_d, u_d) , which is not necessarily straightforward in practice. This section thus proposes one approach to directly compute the robust control input (6) of Theorem 1 in real-time via imitation learning. Note that all the following discussions are also applicable to systems with a known Lyapunov function due to Theorem 2.

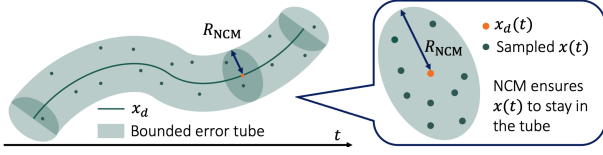


Fig. 2. Illustration of state sampling in robust bounded error tube.

A. Sampling of Expert Demonstrations

We generate expert demonstration data using existing centralized motion planners including the one we use in this work [17]. Since the dynamics is perturbed by $d(x, t)$ as in (1), we sample target trajectories by solving the following bounded error tube-based motion planning problem:

$$\min_{x, u} c_1 \int_0^T \|u(t)\| dt + c_2 \int_0^T P(x(t), u(t), t) dt \quad (12)$$

$$\text{s.t. } \dot{x} = f(x, t) + B(x, t)u \text{ and } x \in \tilde{\mathcal{X}} \quad (13)$$

where $c_1 > 0$, $c_2 \geq 0$, $P(x(t), u(t), t)$ is some performance-based cost function, and $\tilde{\mathcal{X}}$ is robust admissible state space defined as $\tilde{\mathcal{X}} = \{x \in \mathbb{R}^n | \forall \xi \in \{\xi | \|x - \xi\| \leq \lim_{t \rightarrow \infty} R_{\text{NCM}}(t)\}, \xi \in \mathcal{X}\}$ with \mathcal{X} being admissible state space for the unperturbed system. Note that $R_{\text{NCM}}(t)$ is given in (8) (and in (11) for systems with a known Lyapunov function).

Lemma 2: Consider the perturbed system (1) and suppose that $x_d(0) = x(0)$. If (x_d, u_d) is given by (12), then the NCM-CLF control (6) of Theorem 1 ensures that the perturbed solution x stays within the admissible state space \mathcal{X} , i.e., $x \in \mathcal{X}, \forall t$.

Proof: The NCM-CLF control with the relation $x_d(0) = x(0)$ guarantees $\|x(t) - x_d(t)\| \leq \lim_{t \rightarrow \infty} R_{\text{NCM}}(t), \forall t$ by (8) of Theorem 1. Since $x_d \in \tilde{\mathcal{X}}$, we have that $\forall \xi \in S(x_d) = \{\xi | \|x_d - \xi\| \leq \lim_{t \rightarrow \infty} R_{\text{NCM}}(t), \xi \in \mathcal{X}\}$. These indicate that $x \in S(x_d)$ and thus $x \in \mathcal{X}$. ■

Therefore, we utilize (12) for generating expert demonstrations in N random environments, $\{(x_d, u_d)\}_{i=1}^N$, based on the result of Lemma 2. The same argument holds for the Lagrangian systems due to Theorem 2.

B. Robust Control Inputs Sampling and Imitation Learning

The novelty of our approach lies in modeling the robust control policy (6) that maps x to u , instead of the feedforward policy that maps x_d to u_d . To this end, we sample state and robust control input pairs (x, u) using the target trajectories $\{(x_d, u_d)\}_{i=1}^N$ given by (12) as follows.

We first sample artificially perturbed states x in the tube $\mathcal{B}(x_d)$ given as $\mathcal{B}(x_d) = \{\xi \in \mathbb{R}^n | \|\xi - x_d\| \leq \lim_{t \rightarrow \infty} R_{\text{NCM}}(t)\}$ as depicted in Fig. 2. Since any perturbed state trajectory $x(t)$ with $x_d(0) = x(0)$ satisfies $x \in \mathcal{B}(x_d)$ and $x \in \mathcal{X}$ as long as it is controlled by the NCM-CLF (6) as shown in (8) of Theorem 1 and Lemma 2, respectively, we then sample u by solving (6) with such $x \in \mathcal{B}(x_d)$ and (x_d, u_d) of (12). For each of N target trajectories $\{(x_d, u_d)\}_{i=1}^N$, we compute M robust control inputs, resulting in NM training samples $\{(x, u)\}_{j=1}^{NM}$. We propose a novel

imitation learning-based robust and optimal controller in the following proposition.

Proposition 1: The imitation learning-based NCM-CLF control of Theorem 1 is a neural network model for approximating state-robust control input training data $\{(x, u)\}_{j=1}^{NM}$, sampled based on Lemma 2 and Sec. III-B (see Fig. 2). The architecture of this framework is summarized in Fig. 1.

Remark 3: Since (6) is modeled by a neural network in Proposition 1, using local observations in training also enables its decentralized implementation accounting for centralized global solutions [8], [30]. This property will be demonstrated in Sec. V to enable real-time implementation of Proposition 1.

IV. LEARNING-BASED AUTONOMOUS GUIDANCE WITH ROBUSTNESS, OPTIMALITY, AND SAFETY GUARANTEES (LAG-ROS)

The final component we add to the proposed imitation learning-based NCM-CLF control law of Proposition 1 is provable safety guarantee even for systems perturbed by bounded disturbances (1). To this end, we utilize a recently-developed concept of learning-based MPC [27]. The key difference of this approach in Proposition 2 from existing MPC frameworks is that we can select its time horizon much smaller for online implementation depending on the relative degree of safety constraints (see Corollary 1), as it attempts to find u that minimizes the deviation from the learning-based robust and optimal controller u_L of Proposition 1, $\int \|u - u_L\|^2 dt$, instead of $\int \|u\|^2 dt$, along with hard safety constraints.

Proposition 2: Let u_L denote the learning-based NCM-CLF control of Proposition 1, $u = u_d + K^*(x, x_d, t)e$, approximately modeled by a neural network. The Learning-based Autonomous Guidance of Nonlinear Systems with Robustness, Optimality, and Safety (LAG-ROS) control input during $t \in [t_i, t_{i+1})$ is given by u_i^* as a result of the following optimization problem, constructed to minimize the deviation of u_i^* from $u_L(t_i)$:

$$u_i^*, u_{i+1}^*, \dots, u_{i-1}^* = \arg \min_{u_k \in \mathbb{R}^m, \forall k} \sum_{k=i}^{i-1} \|u_k - u_L(t_k)\|^2 \quad (14)$$

$$\text{s.t. } \dot{\bar{x}} = f(\bar{x}, t) + B(\bar{x}, t)u_k, \forall t \in [t_k, t_{k+1}), \quad (15)$$

$$\bar{x}(t_i) = x(t_i), \text{ and } \bar{x}(t_{k+1}) \in \tilde{\mathcal{X}}_k, \forall k = i, \dots, i-1 \quad (16)$$

where $x(t_i)$ is the perturbed solution of (1) observed at $t = t_i$, $\tilde{\mathcal{X}}_k = \{q \in \mathbb{R}^n | \forall \xi \in \{\xi | \|q - \xi\| \leq \bar{d}\Delta t_i, \xi \in \mathcal{X}(t_{k+1})\}, \Delta t_i = t_{i+1} - t_i, \mathcal{X}$ is admissible safe state space, and $\bar{d} = \sup_{x, t} \|d(x, t)\|$ as defined in (1). If I_i is selected small enough to make (14) solvable online at $t = t_i$, the LAG-ROS is implementable in real-time and its perturbed solution x governed by (1) stays in \mathcal{X} for $t \in [t_i, t_{i+1})$.

Proof: Integrating (15) and (1) from t_i to t with the constraint $\bar{x}(t_i) = x(t_i)$ of (16) yields $\|x(t) - \bar{x}(t)\| \leq \bar{d}|t - t_i|$. Thus $\bar{x}(t_{i+1}) \in \tilde{\mathcal{X}}_i$ of (16) implies that $x(t_{i+1}) \in \mathcal{X}(t_{i+1})$. Since $|t - t_i| < \Delta t_i$ for $t \in [t_i, t_{i+1})$, x of (1) stays in \mathcal{X} for $t \in [t_i, t_{i+1})$ as desired. ■

The following corollary is useful for dramatically reducing computational complexity of Proposition 2 for real-time implementation.

Corollary 1: The optimization problem (14) of Proposition 2 with $I_i = i + 1$ is convex/quadratic if the robust safe set $\tilde{\mathcal{X}}_i$ of (16) is convex/quadratic.

Proof: Since $\bar{x}(t_{i+1})$ is affine in u_i due to (15) and (16), $\bar{x}(t_{i+1}) \in \tilde{\mathcal{X}}_i$ is convex/quadratic if $\tilde{\mathcal{X}}_i$ is convex/quadratic [36]. ■

Corollary 1 indicates that a wide range of safety constraints such as affine state constraints (e.g. $x_{\min} \leq x \leq x_{\max}$) and collision avoidance [17], can be incorporated into the LAG-ROS framework without destroying convex structure for computational efficiency. We demonstrate its performance and its real-time implementability later in Sec. V.

Remark 4: The safety part of the LAG-ROS approach in Proposition 2 is not intended to supersede but can be replaced by other existing state-of-the-art control techniques for safety-critical systems, depending on the application of interest. This includes [37], which utilizes control barrier functions for ensuring safety of nonlinear dynamical systems under input disturbances (i.e. $\dot{x} = f(x) + B(x)(u + d)$). In general, safety can be augmented on top of the learning-based NCM-CLF control u_L in Proposition 1 as follows:

$$u^*(t_i) = \arg \min_{u \in \mathbb{R}^m} \|u - u_L(t_i)\|^2 \quad (17)$$

$$\text{s.t. safety constraints given by existing techniques.} \quad (18)$$

Note that input constraints $u \in \mathcal{U}$ can be incorporated in (6), (12), (14), and (17) following the same proof.

The pseudocode to construct and implement the LAG-ROS control is presented in Algorithm 1. We train learning-based NCM-CLF control of Proposition 1 offline, and then implement it online with a safety constraint as in Proposition 2 and Corollary 1.

V. SIMULATION

Our proposed LAG-ROS framework is demonstrated using multiple motion planning problems under external disturbances (<https://github.com/astrohiro>). CVXPY [38] with the MOSEK solver [39] is used to solve optimization problems. In this section, we use a neural network with 3 layers and 100 neurons for imitation learning in Proposition 1, and 3 layers and 32 neurons for deep set-based global-to-local safe autonomy synthesis [8], [30]. Note that the computational time of each framework is measured for the Macbook Pro laptop (2.2 GHz Intel Core i7, 16 GB 1600 MHz DDR3 RAM), and simulation results are the average over 50 simulations for each random environment and disturbance realization.

A. Cart-Pole Balancing

We first utilize the cart-pole balancing task in Fig. 3 for illustrating how to apply the LAG-ROS motion planner in practice. Its equation of motion is given in [24], [31], and its parameters are given as $g = 9.8$, $m_c = 1.0$, $m = 0.1$, $\mu_c = 0.5$, $\mu_p = 0.002$, and $l = 0.5$.

The objective of this task is selected to drive the system state, $x = [p, \theta, \dot{p}, \dot{\theta}]^\top$ in Fig. 3, to $x = [p_f, 0, 0, 0]^\top$ in 10

Algorithm 1: LAG-ROS Algorithm

1. OFFLINE PHASE

Inputs : Random environments $\{\mathcal{E}_i\}_{i=1}^N$
 NCM of [25]/known Lyapunov function
 Motion planner \mathcal{P}

Outputs: Learning-based control u_L of Proposition 1
for $i \leftarrow 1$ **to** N **do**

Solve (12) for \mathcal{E}_i using \mathcal{P} and obtain $(x_d^{(i)}, u_d^{(i)})$
 Sample M robust NCM-CLF control inputs
 $\{(x_j^{(i)}, u_j^{(i)})\}_{j=1}^M$ based on Lemma 2 and
 Sec. III-B (see Fig. 2)

Model $\{(x_j^{(i)}, u_j^{(i)})\}_{j=1}^M\}_{i=1}^N$ by a neural network as in Proposition 1 (see Fig. 1) and save it as u_L

2. ONLINE PHASE

Inputs : Current state and time $(x(t), t)$
 Learning-based control u_L of Proposition 1

Outputs: LAG-ROS control input of Proposition 2
 Determine I_i of (14) small enough based on current computational power at time t
 Solve (14) of Proposition 2 and obtain $u(t)$

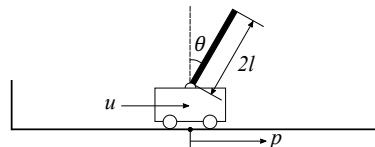


Fig. 3. Cart-pole balancing task.

seconds with minimum $\mathcal{L}2$ control effort under bounded disturbances ($\sup \|d\| = 2.0$), where p_f is a random terminal position at each episode. To this end, we sample target trajectories (x_d, u_d) for 100 random initial and terminal states (10000 training samples) using the centralized motion planner in [17], and construct the LAS-ROS neural net as explained in Proposition 1 using the NCM [25] as a CLF. Its performance is compared with the global robust MPC-based controller [16], learning-based controller which models the feedforward (FF) control policy $u_d \mapsto x_d$ [8], and robust NCM controller [25].

As summarized in Table I, the LAG-ROS objective value $\int_0^{10} \|u(t)\|^2 dt$ is only 9.5% larger than that of the robust MPC with 42.2% smaller computational time. Since we select the time interval of control inputs to be $\Delta t = 0.1$ (s), the LAG-ROS is indeed implementable online while the robust MPC demands higher computational power to solve its optimization routine within $\Delta t = 0.1$ (s). Also, due to the robustness and optimality properties of the LAG-ROS, it achieves 100.0% success rate even under external disturbances unlike the learning-based FF control (40.0% success rate), and gives 61.3% smaller $\int_0^{10} \|u(t)\|^2 dt$ than that of the NCM robust control.

B. Multi-Agent Nonlinear Motion Planning

We next consider motion planning and collision avoidance of multiple spacecraft simulators [32] in a cluttered

TABLE I
CONTROL PERFORMANCES FOR CART-POLE BALANCING (AVERAGED OVER 50 SIMULATIONS WITH $\sup \|d\| = 2.0$).
NOTE THAT COMPUTATIONAL TIME SHOULD BE LESS THAN CONTROL TIME INTERVAL $\Delta t = 0.1$ (s) FOR REAL-TIME IMPLEMENTATION.

	Success rate out of 50 trials (%)	$\mathcal{L}2$ control effort ($\int_0^{10} \ u(t)\ dt$)	Computational time per time step (s)
(a) Learning-based FF [8]	4.0000×10	5.3821×10^2 (7.2840 \times 10% of (d))	7.1569×10^{-4}
(b) Robust NCM [25]	1.0000×10^2	2.0888×10^3 (2.8270 \times 10 ² % of (d))	4.0522×10^{-2}
(c) LAG-ROS	1.0000×10^2	8.0909×10^2 (1.0950 \times 10 ² % of (d))	3.9814×10^{-2}
(d) Robust MPC [14]	1.0000×10^2	7.3889×10^2 (1.0000 \times 10 ² % of (d))	1.3990×10^{-1}

environment with external disturbances, where the agents are supposed to perform tasks based only on local observations and thus centralized motion planners are not implementable in real-time unlike in the previous setting. Note that its equation of motion is given in [32] and all of its parameters are normalized to 1. The goal of each agent is to reach a random target position with minimum $\mathcal{L}2$ control effort while avoiding collision with a random number of multiple circular obstacles (0.5m in radius) and of other spacecraft within 45s under bounded disturbances ($\sup \|d\| = 0.8$). Communication radius for local observations is selected as 2.0m. We sample training data for 15 random environments (13500 training samples) using the centralized motion planner with a robust tube constraint [16]–[18] as illustrated in Fig. 2. When training the LAG-ROS, the localization technique [8] is used for the sake of its distributed implementation (see Remark 3). We again use the NCM [25] as a CLF for its robustness property.

Figure 4 shows the trajectories of each spacecraft under unknown external disturbances for the learning-based FF control [8], robust MPC, LAG-ROS, and the global solution given by the centralized motion planner for comparison. Table II shows that the LAG-ROS is able to compute its optimal control input in real-time (9.5559×10^{-2} s) even with the safety filter of Proposition 2, as it is less than the control time interval $\Delta t = 0.1$ (s) of this problem. It achieves more than 71.4% improvement in its control performance and 111.3% improvement in its success rate compared with the robust MPC, even when the learning-based FF control ends up with only 2.6% success rate. This is primarily due to the fact that the LAG-ROS approximates the global robust optimal solution, while the learning-based FF lacks in robustness and the robust MPC only considers local optimality. We remark that a slightly better onboard computer is required for the robust MPC as its computational time 2.2400×10^{-1} s is greater than $\Delta t = 0.1$ (s). Also, the LAG-ROS objective value is only 22.7% larger than that of the global robust motion planner, which indicates that it can approximate the robust optimal solution in real-time only with local observations. These overall trends are the same for other sizes of disturbances as can be seen in Fig. 7: the LAG-ROS keeps more than 90% success rate for all the disturbances when averaged over 50 simulations, with $\mathcal{L}2$ control effort smaller than 2.0 times that of the global solution unlike the learning-based FF and real-time MPC.

C. Spacecraft Reconfiguration in Low Earth Orbit (LEO)

We finally consider the problem of spacecraft reconfiguration in LEO as an example of systems equipped with a known Lyapunov function. The dynamical system is presented in [40] accounting for J_2 and atmospheric drag perturbations. Since it can be expressed as a fully-actuated Lagrangian system [17], we can design a Lyapunov function by its inertia matrix [29] and use it for the LAG-ROS construction of Proposition 2 due to Theorem 2. The spacecraft communication radius for local observations is selected as 2.0km, which prevents the use of global motion planners. The agents are expected to perform reconfiguration within 75s under bounded disturbances ($\sup \|d\| = 1.0$).

Table III shows the simulation results with external disturbances given in Fig. 6 for the robust MPC, learning-based FF, LAG-ROS, and global motion planner [17]. The LAG-ROS achieves only a 5.9% increase in the objective value even with the computational time less than $\Delta t = 0.1$ (s), which makes it implementable in real-time. Again, a slightly better onboard computer is required for the robust MPC as its computational time 1.5357×10^{-1} s is greater than $\Delta t = 0.1$ (s). Since the LAG-ROS models the global robust optimal solution, it also attains more than a 28.4% decrease in the objective value when compared with the robust MPC, even though the success rate of learning-based FF control is only 2.6% due to external disturbances. These results indicate that the LAG-ROS can be applied with known Lyapunov functions constructed utilizing a special structure of underlying dynamical systems [29], [41] for the sake of a learning-based robustness guarantee. These trends are the same for other sizes of disturbances as can be seen in Fig. 7: the LAG-ROS keeps more than 98% success rate for all the disturbances when averaged over 50 simulations, with $\mathcal{L}2$ control effort smaller than 2.4 times that of the global solution unlike the learning-based FF and real-time MPC.

VI. CONCLUSION

In this work, we propose the LAG-ROS, a real-time implementable safe and optimal motion planner with a learning-based robustness guarantee. It utilizes imitation learning and contraction theory to model a tube-based robust feedback motion planner, constructed using an NCM (or a known Lyapunov function if available [29]) as a CLF. Simulation results demonstrate that it outperforms existing state-of-the-art real-time motion planners even in decentralized multi-agent settings with external disturbances. We remark that

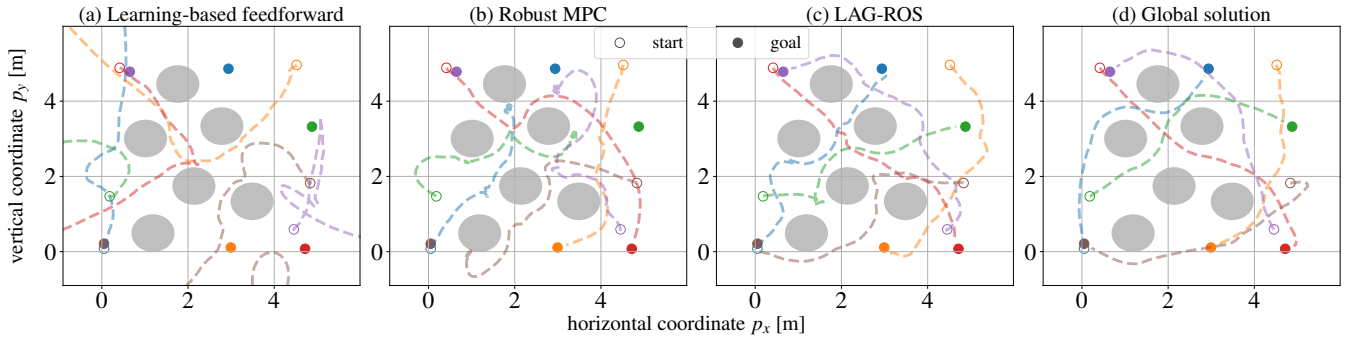


Fig. 4. Spacecraft trajectories for baselines (a) [8] & (b) [16] and for (c) LAG-ROS, where (d) shows the global solution computed offline assuming each agent have access to global information. The LAG-ROS achieves the highest success rate with the control effort closest to that of the global solution.

TABLE II

CONTROL PERFORMANCES FOR MULTI-AGENT SPACECRAFT MOTION PLANNING (AVERAGED OVER 50 SIMULATIONS WITH $\sup \|d\| = 0.8$). NOTE THAT COMPUTATIONAL TIME SHOULD BE LESS THAN CONTROL TIME INTERVAL $\Delta t = 0.1$ (S) FOR REAL-TIME IMPLEMENTATION.

	Success rate out of 50 trials (%)	$\mathcal{L}2$ control effort ($\int_0^{45} \ u(t)\ dt$)	Computational time per time step (s)
(a) Learning-based FF [8]	2.5641	2.1787×10^3 ($1.2164 \times 10^2\%$ of (d))	8.9623×10^{-2}
(b) Robust MPC [16]	4.2628×10	7.6912×10^3 ($4.2943 \times 10^2\%$ of (d))	2.2400×10^{-1}
(c) LAG-ROS	9.0064×10	2.1971×10^3 ($1.2267 \times 10^2\%$ of (d))	9.5559×10^{-2}
(d) Global solution	1.0000×10^2	1.7910×10^3 ($1.0000 \times 10^2\%$ of (d))	1.2064×10^3 (offline computation)

TABLE III

CONTROL PERFORMANCES FOR MULTI-AGENT SPACECRAFT RECONFIGURATION IN LEO (AVERAGED OVER 50 SIMULATIONS WITH $\sup \|d\| = 1.0$). NOTE THAT COMPUTATIONAL TIME SHOULD BE LESS THAN CONTROL TIME INTERVAL $\Delta t = 0.1$ (S) FOR REAL-TIME IMPLEMENTATION.

	Success rate out of 50 trials (%)	$\mathcal{L}2$ control effort ($\int_0^{75} \ u(t)\ dt$)	Computational time per time step (s)
(a) Learning-based FF [8]	3.0000	1.4636×10^2 ($1.0250 \times 10^2\%$ of (d))	7.6204×10^{-2}
(b) Robust MPC [16]	1.0000×10^2	2.1109×10^2 ($1.4784 \times 10^2\%$ of (d))	1.5357×10^{-1}
(c) LAG-ROS	1.0000×10^2	1.5119×10^2 ($1.0589 \times 10^2\%$ of (d))	8.3024×10^{-2}
(d) Global solution	1.0000×10^2	1.4278×10^2 ($1.0000 \times 10^2\%$ of (d))	7.4810×10^2 (offline computation)

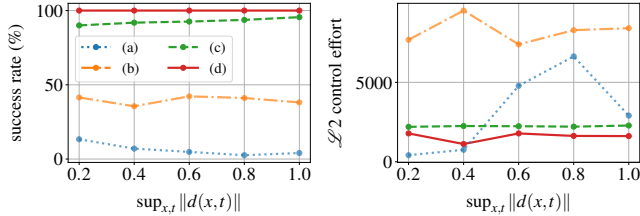


Fig. 5. Control performances versus $\sup_{x,t} \|d(x,t)\|$ for multi-agent spacecraft motion planning (averaged over 50 simulations). (a)–(d) are as in Table II.

other types of disturbances can be incorporated in this framework using [23] for stochastic systems and [24] for parametric uncertain systems.

Acknowledgments: This work was funded by the Jet Propulsion Laboratory, California Institute of Technology, and benefited from discussions with Julie Castillo-Rogez, Michel D. Ingham, and Jean-Jacques E. Slotine.

REFERENCES

- [1] R. S. Sutton and A. G. Barto, *Reinforcement Learning: An Introduction*. MIT Press, 1998.
- [2] D. P. Bertsekas and J. N. Tsitsiklis, *Neuro-Dynamic Programming*. Athena Scientific, 1996.
- [3] N. M. Boffi, S. Tu, N. Matni, J.-J. E. Slotine, and V. Sindhvani, “Learning stability certificates from data,” in *CoRL*, Nov. 2020.
- [4] D. Ho and J. C. Doyle, “Robust model-free learning and control without prior knowledge,” in *IEEE CDC*, 2019, pp. 4577–4582.
- [5] M. Everett, Y. F. Chen, and J. P. How, “Motion planning among dynamic, decision-making agents with deep reinforcement learning,” in *IEEE/RSJ IROS*, 2018, pp. 3052–3059.
- [6] F. Berkenkamp, M. Turchetta, A. Schoellig, and A. Krause, “Safe model-based reinforcement learning with stability guarantees,” in *Adv. Neural Inf. Process. Syst.*, vol. 30. Curran Associates, Inc., 2017, pp. 908–918.
- [7] J. Carius, F. Farshidian, and M. Hutter, “Mpc-net: A first principles guided policy search,” *IEEE Robot. Automat. Lett.*, vol. 5, no. 2, pp. 2897–2904, 2020.
- [8] B. Rivière, W. Hönig, Y. Yue, and S. Chung, “GLAS: Global-to-local safe autonomy synthesis for multi-robot motion planning with end-to-end learning,” *IEEE Robot. Automat. Lett.*, vol. 5, no. 3, pp. 4249–4256, 2020.
- [9] J. Ho and S. Ermon, “Generative Adversarial Imitation Learning,” in *Adv. Neural Inf. Process. Syst.*, D. Lee, M. Sugiyama, U. Luxburg, I. Guyon, and R. Garnett, Eds., vol. 29. Curran Associates, Inc., 2016, pp. 4565–4573.
- [10] A. Gupta, J. Johnson, L. Fei-Fei, S. Savarese, and A. Alahi, “Social GAN: Socially acceptable trajectories with generative adversarial networks,” in *IEEE/CVF Conf. Comput. Vision Pattern Recognit.*, 2018, pp. 2255–2264.
- [11] A. Kuefer, J. Morton, T. Wheeler, and M. Kochenderfer, “Imitating

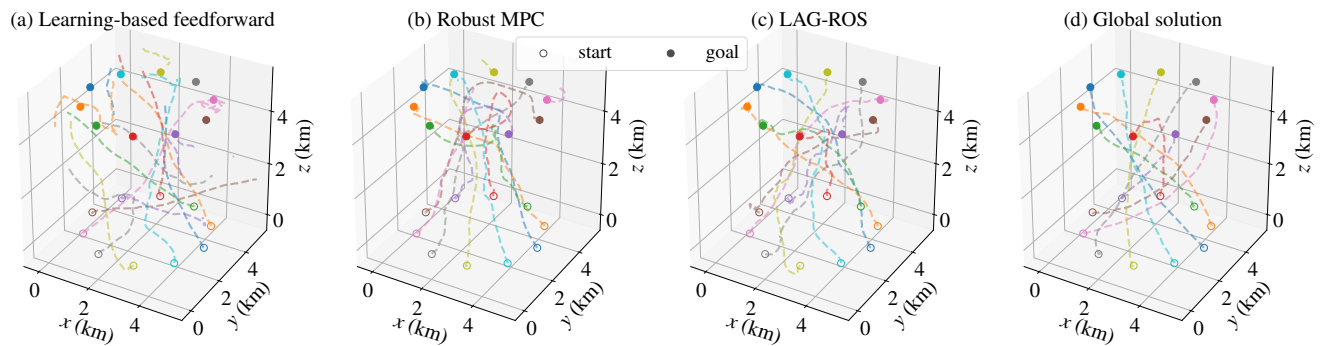


Fig. 6. Spacecraft reconfiguration in LEO with baselines (a) [8] & (b) [16] and for (c) LAG-ROS, where (d) shows the solution computed offline assuming global environment observations. The LAG-ROS achieves the highest success rate with the control effort closest to that of the global solution.

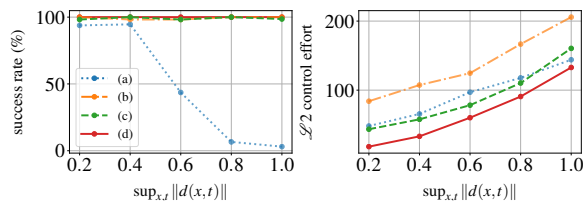


Fig. 7. Control performances versus $\sup_{x,t} \|d(x,t)\|$ for spacecraft reconfiguration in LEO (averaged over 50 simulations). (a)–(d) are as in Table III.

driver behavior with generative adversarial networks,” in *IEEE Intell. Vehicles Symp.*, 2017, pp. 204–211.

- [12] S. Ross and D. Bagnell, “Efficient reductions for imitation learning,” in *13th Int. Conf. Artif. Intell. Statist.*, ser. Proc. Mach. Learn. Res., vol. 9, May 2010, pp. 661–668.
- [13] A. Bemporad and M. Morari, “Robust model predictive control: A survey,” in *Robustness in identification and control*. London: Springer London, 1999, pp. 207–226.
- [14] D. Mayne, M. Seron, and S. Raković, “Robust model predictive control of constrained linear systems with bounded disturbances,” *Automatica*, vol. 41, no. 2, pp. 219 – 224, 2005.
- [15] S. Singh, A. Majumdar, J.-J. E. Slotine, and M. Pavone, “Robust online motion planning via contraction theory and convex optimization,” in *IEEE ICRA*, May 2017, pp. 5883–5890.
- [16] D. Q. Mayne, E. C. Kerrigan, E. J. van Wyk, and P. Falugi, “Tube-based robust nonlinear model predictive control,” *Int. J. Robust Nonlinear Control*, vol. 21, no. 11, pp. 1341–1353, 2011.
- [17] D. Morgan, S.-J. Chung, and F. Y. Hadaegh, “Model predictive control of swarms of spacecraft using sequential convex programming,” *J. Guid. Control Dyn.*, vol. 37, no. 6, pp. 1725–1740, 2014.
- [18] J. Schulman, Y. Duan, J. Ho, A. Lee, I. Awwal, H. Bradlow, J. Pan, S. Patil, K. Goldberg, and P. Abbeel, “Motion planning with sequential convex optimization and convex collision checking,” *Int. J. Robot. Res.*, vol. 33, no. 9, pp. 1251–1270, 2014.
- [19] Y. K. Nakka, A. Liu, G. Shi, A. Anandkumar, Y. Yue, and S. J. Chung, “Chance-constrained trajectory optimization for safe exploration and learning of nonlinear systems,” *IEEE Robot. Automat. Lett.*, vol. 6, no. 2, pp. 389–396, 2021.
- [20] E. Sontag, “A Lyapunov-like characterization of asymptotic controllability,” *SIAM J. Control Optim.*, vol. 21, no. 3, pp. 462–471, 1983.
- [21] E. D. Sontag, “A ‘universal’ construction of Artstein’s theorem on nonlinear stabilization,” *Syst. Control Lett.*, vol. 13, no. 2, pp. 117 – 123, 1989.
- [22] H. K. Khalil, *Nonlinear Systems*, 3rd ed. Prentice-Hall, 2002.
- [23] H. Tsukamoto, S.-J. Chung, and J.-J. E. Slotine, “Neural stochastic contraction metrics for learning-based control and estimation,” *IEEE Control Syst. Lett.*, vol. 5, no. 5, pp. 1825–1830, 2021.
- [24] —, “Learning-based adaptive control via contraction theory,” *Submitted to IEEE Control Syst. Lett.*, Mar. 2021.
- [25] H. Tsukamoto and S.-J. Chung, “Neural contraction metrics for robust estimation and control: A convex optimization approach,” *IEEE Control Syst. Lett.*, vol. 5, no. 1, pp. 211–216, 2021.
- [26] W. Lohmiller and J.-J. E. Slotine, “On contraction analysis for nonlinear systems,” *Automatica*, no. 6, pp. 683 – 696, 1998.
- [27] L. Hewing, K. P. Wabersich, M. Menner, and M. N. Zeilinger, “Learning-based model predictive control: Toward safe learning in control,” *Annu. Rev. Control Robot. Auton. Syst.*, vol. 3, no. 1, pp. 269–296, 2020.
- [28] G. Shi *et al.*, “Neural lander: Stable drone landing control using learned dynamics,” in *IEEE ICRA*, May 2019.
- [29] J.-J. E. Slotine and W. Li, *Applied Nonlinear Control*. Upper Saddle River, NJ: Pearson, 1991.
- [30] M. Zaheer, S. Kottur, S. Ravanbakhsh, B. Póczos, R. R. Salakhutdinov, and A. J. Smola, “Deep sets,” in *Adv. Neural Inf. Process. Syst.*, vol. 30. Curran Associates, Inc., 2017, pp. 3391–3401.
- [31] A. G. Barto, R. S. Sutton, and C. W. Anderson, “Neuronlike adaptive elements that can solve difficult learning control problems,” *IEEE Trans. Syst. Man Cybern.*, vol. SMC-13, no. 5, pp. 834–846, 1983.
- [32] Y. Nakka *et al.*, “A six degree-of-freedom spacecraft dynamics simulator for formation control research,” in *Astrodyn. Special. Conf.*, 2018.
- [33] H. Tsukamoto and S.-J. Chung, “Robust controller design for stochastic nonlinear systems via convex optimization,” *IEEE Trans. Autom. Control*, to appear, Oct. 2021.
- [34] A. Isidori, *Nonlinear Control Systems*, 3rd ed. Berlin, Heidelberg: Springer-Verlag, 1995.
- [35] J.-J. E. Slotine, “Modular stability tools for distributed computation and control,” *Int. J. Adapt. Control Signal Process.*, vol. 17, no. 6, pp. 397–416, 2003.
- [36] S. Boyd and L. Vandenberghe, *Convex Optimization*. Cambridge University Press, Mar. 2004.
- [37] S. Kolathaya and A. D. Ames, “Input-to-state safety with control barrier functions,” *IEEE Control Syst. Lett.*, vol. 3, no. 1, pp. 108–113, 2019.
- [38] S. Diamond and S. Boyd, “CVXPY: A Python-embedded modeling language for convex optimization,” *J. Mach. Learn. Res.*, 2016.
- [39] MOSEK ApS, *MOSEK Optimizer API for Python 9.0.105*, 2020.
- [40] D. Morgan, S.-J. Chung, L. Blackmore, B. Acikmese, D. Bayard, and F. Y. Hadaegh, “Swarm-keeping strategies for spacecraft Under J2 and atmospheric drag perturbations,” *J. Guid. Control Dyn.*, vol. 35, no. 5, pp. 1492–1506, 2012.
- [41] I. R. Manchester and J.-J. E. Slotine, “Control contraction metrics: Convex and intrinsic criteria for nonlinear feedback design,” *IEEE Trans. Autom. Control*, vol. 62, no. 6, pp. 3046–3053, Jun. 2017.